Partitioning of hazardous elements during preparation of high-uranium coal from Rongyang, Guizhou, China

Piaopiao Duan[a,b], Wenfeng Wang[a,b,*], Shuxun Sang[a,b], Fuchang Qian[a,b], Pei Shao[a,b], Xin Zhao[a,c]

[a] Key Laboratory of Coalbed Methane Resource and Reservoir Formation Process, China University of Mining and Technology, Ministry of Education, Xuzhou 221116, China
[b] School of Resources and Geosciences, China University of Mining and Technology, Xuzhou 221116, China
[c] General Prospecting Institute, China National Administration of Coal Geology, Beijing 100039, China

ARTICLE INFO

ABSTRACT

The Late Permian coal from Rongyang Mine in southwestern China is characterized by high content of sulfur (5.44%) and elevated concentrations of trace elements U (70.5 μg/g), V (283 μg/g), Cr (63.2 μg/g), Co (12.8 μg/g), Cu (59.5 μg/g), Se (5.28 μg/g), and Mo (87.5 μg/g). Because of their potential adverse effects on human health and environments, it is important to understand the pathways of these elements during preparation. This study focuses on the distribution of hazardous elements in the size- and density-fractionated samples of this coal. The results indicated that: (1) The minerals in the Rongyang coals are mainly composed of quartz, pyrite, marcasite, calcite, anatase, illite, and kaolinite, along with traces of coquimbite, bassanite, roemerite, gypsum, dolomite, rutile, and siderite. Most of the minerals can be effectively liberated from cleaned coal by gravity separation. (2) Elements U, V, Cr, Co, Cu, Se, and Mo with a high content in the Rongyang coal are derived from exfiltrational hydrothermal fluids during syngenetic or early diagenetic stages, and are associated with inorganic components such as clay minerals, pyrite, anatase, and guadarramite as well as organic components. Selenium mainly occurs in pyrite (particularly epigenetic pyrite) in the coal. (3) Uranium is the easiest to remove through gravity separation (the removability is 68.33%) and has lowest concentration (10.5 μg/g) in the 3–6 mm size fractions compared to the others size fractions. It was also found that uranium cannot be removed through gravity separation completely, due to its association with the organic components and fine-grained minerals. The U concentration in the cleaned coal is still much higher than the average value for world hard coals. The ash from the cleaned coal with particle size of 6–13 mm and < 0.5 mm could be potentially used for industrial extraction of uranium. (4) The minerals that are epigenetic in origin are easily liberated during coal cleaning. Therefore, hazardous elements Co, Ni, Cu, As, Se, Cd, Sb, Hg, Tl, and Pb that are associated with epigenetic pyrite are thus relatively easy to remove, whereas elements V, Cr, and Mo that are evenly distributed in inorganic and organic components, are more difficult to be removed.

1. Introduction

Guizhou Province is the richest province in coal resources in southwestern China, and its coal production accounts for about 50% of the total production of southwestern China (Hu et al., 2005). Along with the economical development, the demand for coals in Guizhou has increased in recent years. However, a series of environmental challenges are produced during coal mining, processing, and utilization of any coal (Dai et al., 2005, 2006; Diehl et al., 2012). Endemic diseases (such as those caused by As, F, and Se) associated with coal untiliaztion in Guizhou have caused concerns (Finkelman and Tian, 2017; Luo et al., 2008). Unlike other elements, uranium is a radioactive element, which

can cause pollution, though it can also be considered as an important resource (Chen et al., 2017; Dai et al., 2015, 2016b, 2017a; Dai and Finkelman, 2017; Huang and Tang, 2002; Wang et al., 2015). The uranium concentration in most coals is low, certainly below the cut-off of economic extraction (e.g., 1000 μg/g in coal ash; Dai and Finkelman, 2017). The uranium concentration in the Rongyang coal is close to the cut-off grade, and therefore, both from the perspective of the environment and resource utilization, it is necessary to understand the partitioning of uranium during coal cleaning.

Distributions of trace elements in coal have been studied in relation to coal preparation methodology, coal rank, and particle size (Cheng et al., 2013; Duan et al., 2017; Feng et al., 2008; Gerald et al., 2000;
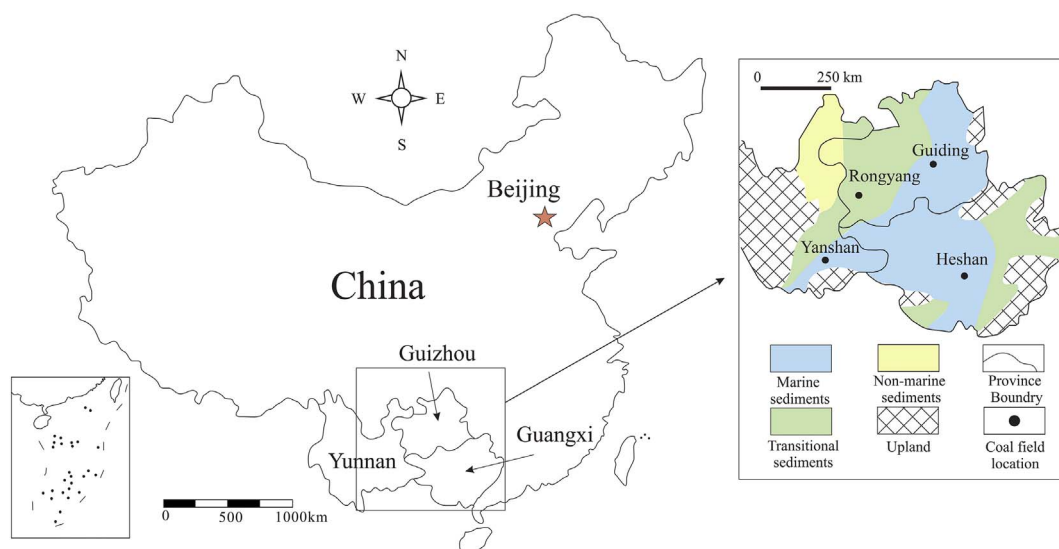
Fig. 1. Paleoenvironment and location of the Rongyang Mine and the Guiding, Yanshan, and Heshan, coalfields in southwestern China (after Dai et al., 2015).

Table 1
Proximate analysis (%), total sulfur and forms of sulfur (%) for the Longtan Formation coal from the Rongyang Mine.

Proximate analysis (%)			Forms of sulfur (%)			
M_{ad}	A_d	V_{daf}	$S_{t,d}$	$S_{p,d}$	$S_{s,d}$	$S_{o,d}$
2.6	19	8.9	5.44	4.19	0.19	1.06

M, moisture; A, ash yield; V, volatile matter; S_t, total sulfur; S_p, pyritic sulfur; S_s, organic sulfur; ad, air-dry basis.

Table 2
Percentages of major-element oxides (%) in the Rongyang coals (on a whole coal air dried basis).

Element oxides	SiO_2	TiO_2	Al_2O_3	Fe_2O_3	MnO_2	MgO	CaO	Na_2O	K_2O
RY	7.26	0.35	4.13	5.98	0.011	0.17	0.23	0.11	0.49
China	8.47	0.33	5.98	4.85	0.015	0.22	1.23	0.16	0.19
CC	0.86	1.07	0.69	1.23	0.75	0.79	0.19	0.68	2.59

RY, the Longtan Formation coals from Rongyang Mine; China, average values of major-element oxides for Chinese coals are from Dai et al. (2012); CC, concentration coefficient, the ratio of Rongyang samples vs. Chinese or world hard coals.

Man et al., 1998; Kolker et al., 2016; Wang et al., 2005, 2006, 2008, 2009; Wang and Qin, 2011; Wang, 2007). High-U coal is not uncommon in southern China. According to Dai et al. (2008, 2013a, 2013b, 2015, 2017b), high-uranium coal is commonly distributed in the Yanshan, Heshan, Fusui, Guiding, and Yishan coalfields of southern China. However, there are few studies concerning the partitioning of trace elements during high-U coal cleaning, and the U distribution in coal preparation products is still unclear. The Late Permian Rongyang

coal is used for electric power generation and it is characterized by high sulfur and U. In this study, the Rongyang coal is selected for the coal preparation experiment and also the geological background and coal petrology characteristics are investigated in the study.

2. Geological setting

The Rongyang Mine is located near the town of Xiashan in Xingren County, Guizhou Province, southwestern China (Fig. 1).

The strata in the mine area include the Upper Permian Longtan and Changxing Formations as well as Quaternary sediments. The mine is located in the Qianbei Uplift of the Yangzi Platform, in the central region where shearing from rotation along the Liupanshui Fault has caused some deformation. However, there are no major faults in the study area and the general geological structure is rather simple compared with other coalfields in southwestern China (China Coal Geology Bureau, 1996; Dai et al., 2016a). The coal-bearing stratum in the mine field is the Upper Permian Longtan Formation, which has a disconformity contact with the underlying middle Permian Maokou Formation. It belongs to marine-terrigenous facies sedimentation (Fig. 1). The Longtan Formation is mainly composed of siltstone, chert, limestone, mudstone, shale, and coal seams, and contains fossils including brachiopods, pteridophyte, and ferns. The Late Permian Longtan Formation coal is interpreted to have formed in a tidal flat environment on an open carbonate platform (Xu and He, 2003). The thickness of the coal measure strata is about 260 m and the dip of the coal is about 4–8°.

3. Samples and analytical procedures

Coal samples from the Longtan Formation were taken from the mine face at the Rongyang Mine. The coal sample was manually crushed to

Table 3
Percentages major-element oxides (%) in coal separation products of different particle sizes (on a whole coal air dried basis).

Particle size (mm)	Coal separation products	SiO_2	TiO_2	Al_2O_3	Fe_2O_3	MgO	CaO	Na_2O	K_2O	P_2O_5	SO_3
< 0.5	Cleaned coal	4.99	0.44	2.04	2.71	0.16	0.197	–	0.279	0.359	9.56
	Middlings	8.9	0.39	2.99	7.82	0.09	0.252	0.12	0.406	0.036	16.16
	Feed coal	9.09	0.38	4.41	10.93	0.15	0.646	0.11	0.567	0.058	20.28
6–13	Cleaned coal	5.94	0.44	3.44	3.12	0.13	0.079	0.11	0.449	0.02	9.07
	Middlings	8.51	0.39	4.70	6.71	0.17	0.32	0.13	0.639	0.018	13.63
	Gangue	16.66	1.67	12.90	13.31	0.39	0.221	0.24	1.300	0.037	21.98
	Feed coal	9.73	0.78	6.49	6.90	0.22	0.138	0.18	0.785	0.024	14.23

–, no data.

Table 4
Concentrations of trace elements (μg/g)[a] in the Rongyang coals (on a whole coal air dried basis).

Elements	F	V	Cr	Co	Ni	Cu	As	Se	Mo	Sb	Ba	Hg	U
RY	32.72	283	62.3	12.8	< 46	59.5	6.3	5.28	87.5	0.52	348	0.18	70.5
World	82	25	16	5.1	13	16	9	1.3	2.2	0.92	150	0.1	1.9
CC	0.40	11.32	3.89	2.51	nd	3.72	0.70	4.06	39.77	0.57	2.32	1.80	37.11

[a] Trace elements (except F, As, Se) were determined by neutron activation analysis; World, trace elements for world hard coals are from Ketris and Yudovich (2009).
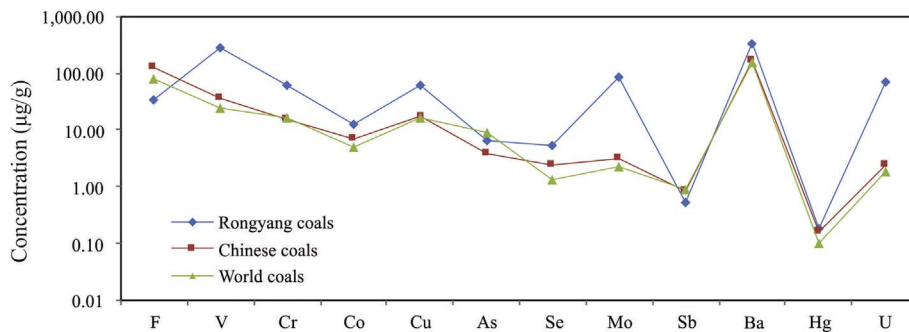

Fig. 2. Concentrations of trace elements (μg/g) in the Rongyang coals, Chinese coals (Dai et al., 2012), and world hard coals (Ketris and Yudovich, 2009).

Table 5
Percentages of minerals in coal separation products with particle size < 0.5 mm and 6–13 mm (%, on a whole coal air dried basis).

| Mineral	< 0.5 mm			Mineral	6–13 mm			
	Feed coal	Cleaned coal	Middlings		Feed coal	Cleaned coal	Middlings	Gangue
Quartz	15.00	15.08	7.83	Quartz	4.13	2.11	6.81	5.60
Pyrite	10.99	4.09	4.99	Pyrite	9.65	3.74	14.74	34.13
Marcasite	4.46	0.47	0.87	Marcasite	1.32	0.41	1.50	3.05
Calcite	4.03	0.22	0.22	Calcite	0.00	0.07	0.00	1.51
Anatase	3.48	0.55	0.24	Anatase	0.15	0.18	0.31	2.18
Illite	3.60	0.75	1.71	Illite	3.73	0.73	1.63	6.42
Kaolinite	1.09	0.71	0.50	Kaolinite	1.84	0.21	2.86	3.74
Coquimbite	5.59	0.96	0.63	Coquimbite	0.00	0.00	1.80	9.81
Bassanite	0.00	0.65	0.58	Bassanite	0.44	0.00	0.00	1.20
Roemerite	0.00	0.00	4.24	Roemerite	0.00	0.00	0.00	0.00
Gypsum	0.00	0.00	1.09	Gypsum	0.48	0.00	0.00	1.51
Dolomite	0.00	0.00	0.90	Dolomite	0.00	0.36	0.00	0.00
Rutile	0.00	0.00	0.00	Rutile	0.00	0.10	0.23	0.78
Siderite	0.00	0.00	0.00	Siderite	0.00	0.24	0.00	0.00
Total	48.23	23.48	23.81	Total	21.74	8.14	29.89	69.94
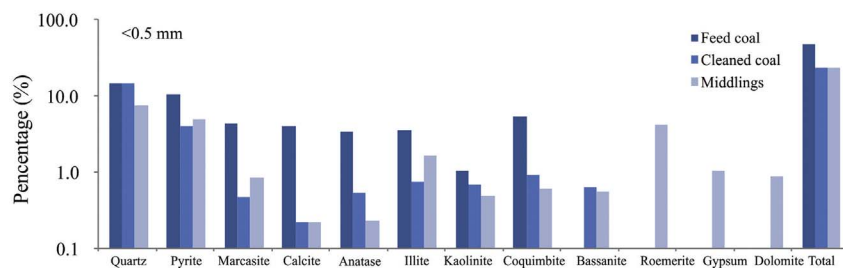
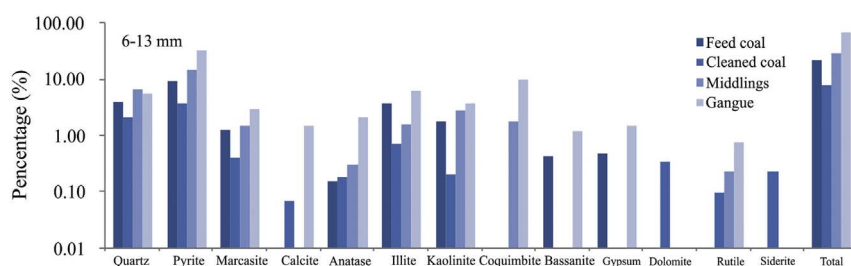**Fig. 3.** Percentages (%) of minerals in coal separation products with a size of < 0.5 mm.

Fig. 4. Percentages (%) of minerals in coal separation products with a size of 6–13 mm.
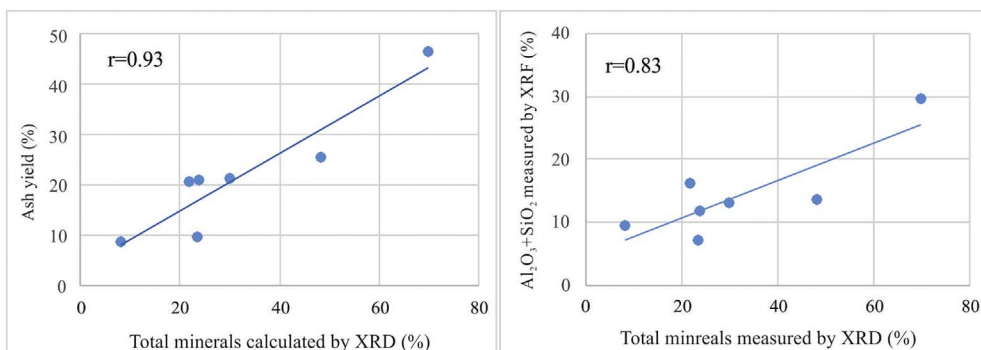
Fig. 5. Correlations of ash yield, $Al_2O_3 + SiO_2$ measured from by XRF and total minerals calculated by XRD for feed coal and coal separation products with particle sizes of < 0.5 mm and 6–13 mm.
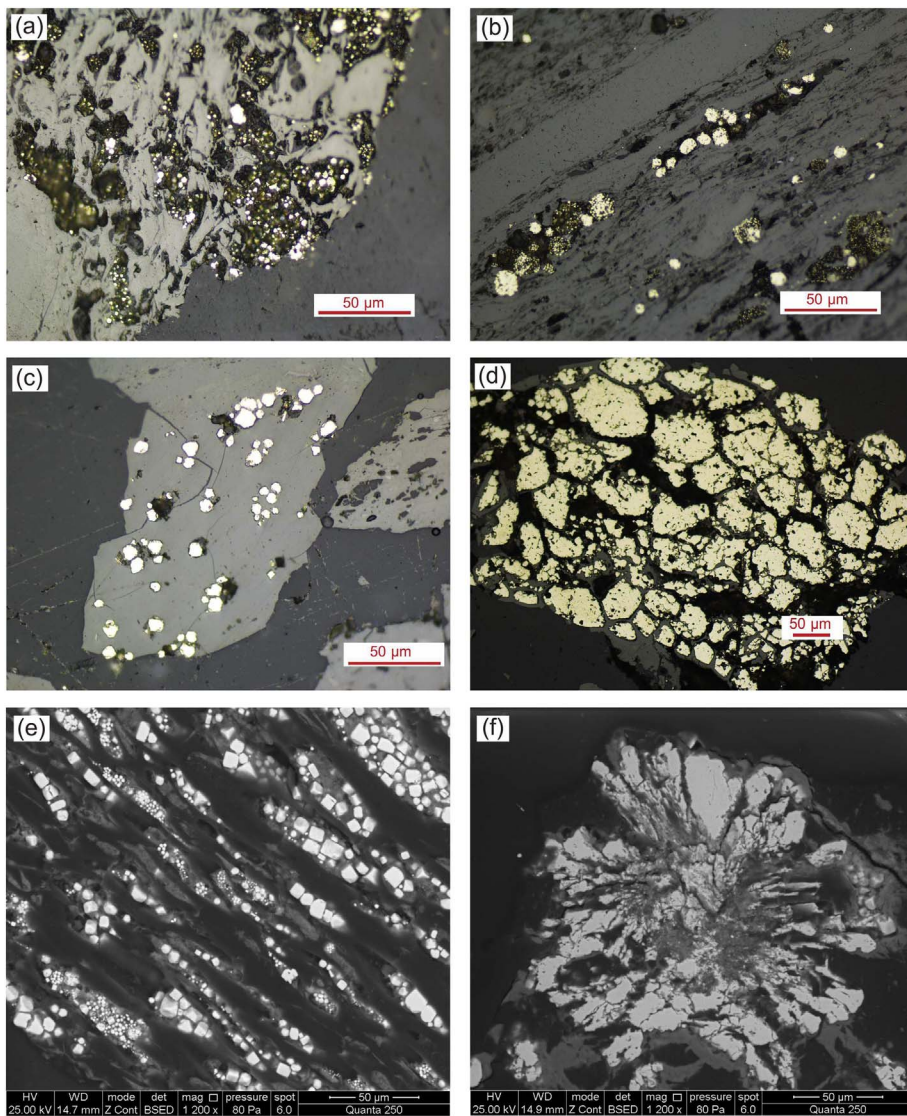

Fig. 6. (a) Pyrites as cell-fillings in cleaned coal with a particle size of 3–6 mm, under reflected light. (b) Framboidal pyrites in middlings with a particle size of 6–13 mm, under reflected light. (c) Granular pyrite in middlings with a size < 0.5 mm, reflected light. (d) Cell-filling pyrite in Rongyang feed coal, reflected light. (e) and (f) Euhedral pyrite and marcasite in Rongyang feed coal, SEM back-scattered electron images.

reduce the particle size to < 13 mm, then the ground products were sieved into four size fractions (6–13 mm, 3–6 mm, 0.5–3 mm, and < 0.5 mm), with a series of stainless steel sieves with mesh apertures of 6, 3, and 0.5 mm. Then each particle size fraction was divided into three coal samples using heavy liquid (zinc chloride) with specific gravity (SG) 1.5 and 1.8 kg/L in density. Finally, two float fractions for densities, < 1.5 and 1.5–1.8 kg/L, and one sink fraction for density, > 1.8 kg/L, were obtained in each particle size, and these three density grade samples were deemed as cleaned coal, middlings, and gangue,

respectively. The centrifuge was used for the float and sink analysis for coal < 0.5 mm in size, and two heavy liquids with specific gravity 1.5 and 1.8 kg/L were used in float and sink analysis in order to separate each coal sample into three subsplits (two float fractions for densities < 1.5 and 1.5–1.8 kg/L [cleaned coal and middlings], and one sink fraction for density > 1.8 kg/L [gangue]).

All samples were crushed and ground to pass 200 mesh (75 μm) for proximate and elemental analyses. Proximate analysis (moisture, ash, and volatile matter) was conducted following ASTM Standards D3173-
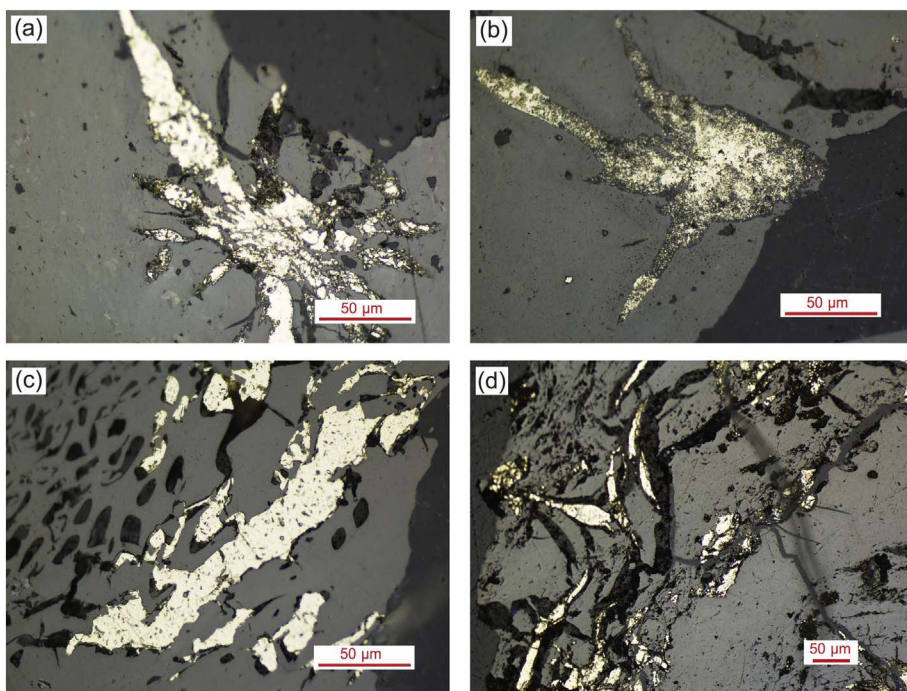
Fig. 7. Reflected light images. (a) Radial pyrite in cleaned coal with a particle size of 3–6 mm. (b) Radial pyrite in feed coal with a particle size of 3–6 mm. (c) Cell- and fracture-filling pyrite in cleaned coal with a particle size of 6–13 mm. (d) Fracture-filling pyrite in middlings with a particle size of 0.5–3 mm.
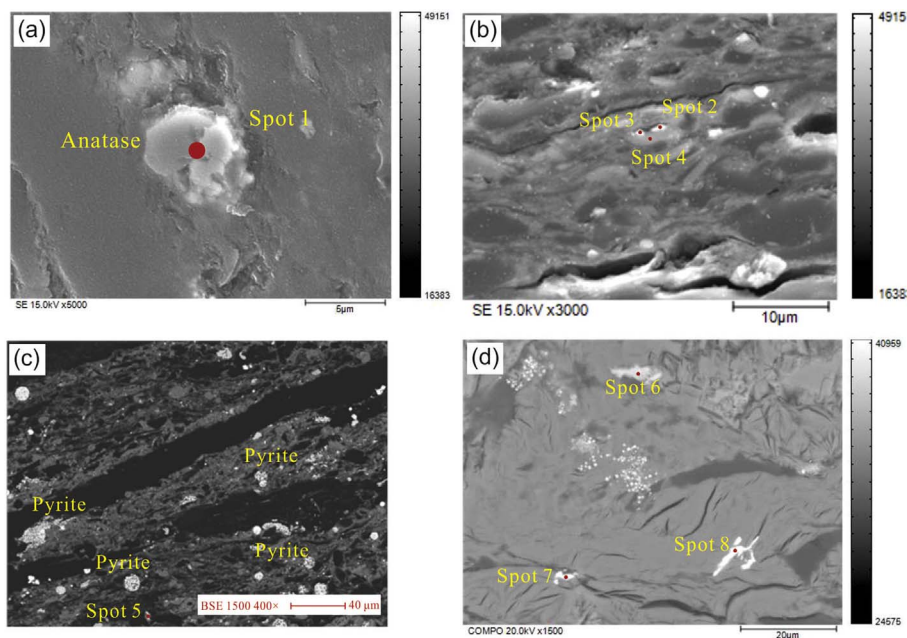

Fig. 8. (a) Anatase in cleaned coal with a particle size of 6–13 mm, secondary electron image. (b) Clay minerals in middlings with a particle size of 6–13 mm, secondary electron image. (c) Clay minerals and pyrites in middlings with a particle size of 6–13 mm, secondary electron image. (d) Clay minerals, pyrites, anatase in middlings with a size of < 0.5 mm, secondary electron image.

11 (2011), D3174-11 (2011), and D3175-11 (2011). The total sulfur and forms of sulfur were determined following ASTM Standards D3177-02 (2002) and D2492-02 (2002).

Mineralogical analyses of samples were performed with optical microscopy, scanning electron microscopy with energy dispersive X-ray (SEM-EDX), X-ray powder diffraction (XRD), and electron microprobe (EPMA). A Leitz MPVIII optical microscopy was also employed for mineral observation, and the images were captured using white-light reflectance microscopy. A scanning electron microscope (SEM, FEI Quanta™ 250), in conjunction with an EDAX energy-dispersive X-ray spectrometer, was used to study the morphology of the minerals. The working distance of the SEM-EDS was between 14 and 20 mm, with a beam voltage of 25 or 30 kV, aperture of 6, and micron spot size of 3.5–5.0. The images were captured with a retractable solid state backscatter electron detector (SSBSED). The coal samples were

analyzed by XRD using a D/max-2500/PC powder diffractometer with Ni-filtered Cu-Kα radiation and a scintillation detector. The XRD patterns were recorded in a 2θ interval of 2.6 to 70° with a step size of 0.01°. In addition, TOPAS 4.2 was used to conduct quantitative mineralogical analysis for X-ray diffractograms of coals. In order to study the U content in the different minerals, the samples were investigated by backscattered electron imaging (BSE) and secondary electron (SE), together with wavelength-dispersive quantitative analysis by EPMA using a 1-μm diameter probe spot.

X-ray fluorescence (XRF) spectrometry (BRUKER S8 TIGER) was used to determine the major-element oxides in the coal ash, including SiO_2, TiO_2, Al_2O_3, Fe_2O_3, MgO, CaO, MnO, Na_2O, and K_2O. Inductively coupled plasma mass spectrometry (Thermal Fisher, X series II ICP-MS) was used to determine trace elements in the samples, except for Hg and F. Prior to ICP-MS analysis, samples were digested using an UltraClave

Table 6
Electron microprobe analysis results of minerals in Fig. 8.

Oxide	Na₂O	MgO	Al₂O₃	SiO₂	P₂O₅	SO₃	Cl	K₂O	CaO	TiO₂	MnO	FeO	ZrO₂	Nb₂O₅	I	La₂O₃	ThO₂	UO₂	Phase identified
In cleaned coal with a particle size of 6–13 mm (Fig. 8a)																			
Spot 1		1.67	8.13		7.75			0.63		78.42		1.98						1.43	Anatase
In middlings with a particle size of 6–13 mm (Fig. 8b)																			
Spot 2	0.38	0.49	14.69	59.03		1.3	0.18	3.6	0.68	5.9		4.08	1.92					7.73	Clay minerals
Spot 3	0.35	0.51	14.84	61.08		2.41	0.27	3.13	0.65	4.9		3.8	1.77		0.22			6.06	Clay minerals
Spot 4	0.23	0.46	14.44	58.04		1.44		2.43	0.6	7.44		4.35	2.36					8.2	Clay minerals
In middlings with a particle size of 6–13 mm (Fig. 8c)																			
Spot 5	0.37	0.19	9.77	32.39		3.09		1.88	0.42	49.12		1.81						0.96	Clay minerals + anatase
In middlings with a size of < 0.5 mm (Fig. 8d)																			
Spot 6	0.19	0.12	3.95	12.73		1.19		0.76	0.31	72.37		4.36	0.82	0.45				2.76	Clay minerals + anatase
Spot 7	0.41	0.45	14.4	47.33		1.47		3.19	0.41	10.79	0.46	12.2	1.63		0.17			7.13	Clay minerals
Spot 8	0.23	0.46	7.61	27.99	0.76	2.92		1.51	0.49	22.05	0.64	15.5	2.25				0.46	17.14	Guadarramite[a] + clay minerals

[a] The mineral probably is guadarramite.

Microwave High Pressure Reactor (Milestone). Coal samples were digested using 5 mL 65% HNO_3 and 2 mL 40% HF, but for the non-coal samples, the reagents include 5 mL 40% HF and 2 mL 65% HNO_3. ICP-MS analysis and sample microwave digestion program for coal and coal-related materials are based on the methods fully described by Dai et al. (2011). Arsenic and Se were determined by ICP-MS equipped with an Automated 3rd Generation Collision Cell Technology (CCT_{ED}). Following procedures by Li et al. (2014), for ICP-CCT-MS determination, the samples were digested using an UltraClave Microwave High Pressure Reactor (Milestone). Arsenic and Se determined by ICP-CCT-MS can effectively diminish the spectral interferences of the Ar-based polyatomic ions $^{40}Ar^{35}Cl$ and $Ar^{38}Ar$ to ^{75}As and ^{78}Se, respectively (Li et al., 2014).

Mercury was determined by method of atomic absorption spectrophotometry using a Milestone DMA-80 analyzer. Fluorine was determined by pyrohydrolysis combined with an ion-selective electrode following ASTM method D 5987–96 (2002).

4. Results and discussion

4.1. Coal chemistry

Proximate analysis, total sulfur and forms of sulfur for the Longtan Formation coal of Rongyang are listed in Table 1. The volatile matter content of the sample is 8.9%, indicating that the Rongyang coal is an anthracite in rank according to the ASTM classification (ASTM Standard D 388–2012).

The Rongyang coal would be classed as a "medium-ash coal", according to the GB 15224.1-2004 (2004) (coals with ash yield 16.02%–29.00% are classified as medium-ash coal). The total sulfur content in the coal is 5.44%, suggesting a high-sulfur coal, according to Chou (2012) and GB/T 15224.2-2004 (2004) (coals with a total sulfur content > 3% are high-sulfur coal). Pyritic sulfur is the dominant form of sulfur.

4.2. Geochemistry

4.2.1. Major element oxides

The concentrations of major element oxides in the Rongyang coal are listed in Table 2. Compared with the average values of major elements for common Chinese coals, only the concentration of K_2O is higher in the Rongyang coal, and the remaining major element oxides are close to those in other common Chinese coals.

As shown in Table 3, in each particle size, the percentage of major-element oxides presented an increasing trend from cleaned coal, middlings to gangue. Compared with the feed coal, the percentage of major-element oxides in cleaned coal and middlings are relatively lower, and gangue has the highest content of major-element oxides.

4.2.2. Trace elements

The concentrations of trace elements in the Rongyang coal are listed in Table 4. Based on the classification of their enrichment proposed by Dai et al. (2015), elements V, Mo, and U are significantly enriched (10 < CC < 100, CC is the ratio of trace elements in samples investigated vs. averages for world hard coals); Cr, Co, Cu, Se, and Ba are slightly enriched in the Rongyang coal (2 < CC < 5); F is depleted (CC < 0.5); As, Sb, and Hg (0.5 < CC < 2) are close to their average values in world hard coals (CC, concentration coefficient). Compared with common Chinese coals (Dai et al., 2012), most trace elements in the Rongyang coal (except F and Sb) have higher elevated concentrations. Fig. 2 shows that the Rongyang coal is characterized by an enrichment of an assemblage of U-V-Cr-Co-Cu-Se-Mo.

4.3. Mineralogy

4.3.1. XRD analysis of coal separation products

Quantitative mineralogical compositions are listed in Table 5. XRD data show that the minerals in the Rongyang coal are mainly composed of quartz, pyrite, marcasite, calcite, anatase, illite, and kaolinite, along with traces of coquimbite, bassanite, roemerite, gypsum, dolomite, rutile, and siderite (Table 5). The total mineral content in feed coal with a particle size < 0.5 mm is much higher than that in feed coal with a size of 6–13 mm. For the fractions with a size of < 0.5 mm, the minerals could be effectively removed from the cleaned coal and middlings by cleaning (Fig. 3 and Table 5). For the fractions with a size of 6–13 mm, the minerals are enriched in middlings and gangue, and were reduced to 8.14% in cleaned coal (Fig. 4 and Table 5), suggesting that most minerals can be removed by gravity separation.

The Fig. 5 shows the correlations of ash yield (listed in Table 7), $Al_2O_3 + SiO_2$ measured by XRF and the percentage of total minerals calculated by XRD and software TOPAS 4.2 for feed coal and coal separation products with particle sizes of < 0.5 mm and 6–13 mm. The total minerals are highly correlated with ash yield and $Al_2O_3 + SiO_2$, indicating that minerals calculated from XRD are compatible with the chemical analyses and proving that the quantifications derived from the XRD data are reliable.

4.3.2. Modes of occurrence of minerals

The optical microscopy and SEM-EDX observations also found that minerals are mainly composed of pyrite, marcasite, and clay minerals. The syngenetic or early-diagenetic pyrite occurs as cell-filling (Fig. 6a, c, d), framboidal (Fig. 6b), and discrete crystal forms in cavities of the organic matter (Fig. 6c, e). Dai et al. (2006) studied the minerals from a Xingren coal and found that epigenetic pyrite was derived from low-temperature hydrothermal fluids. Li and Tang (2005) considered that low-temperature hydrothermal fluid is the main cause of hazardous elements in the coals in western Guizhou. In addition, some pyrites occur as radial (Fig. 7a, b) and fracture-filling (Fig. 7c, d) forms,

Table 7
Percentages of ash (%) and sulfur (%, on a whole coal dry basis), concentrations of trace elements (µg/g, on a whole coal air dried basis) in coal separation products of different particle sizes.

Particle size (mm)	Coal separation products	A_d	$S_{t,d}$	$S_{p,d}$	$S_{s,d}$	$S_{o,d}$	Be	F	V	Cr	Co	Ni	Cu	As	Se	Mo	Cd	Sb	Ba	Hg	Tl	Pb	U
6–13	Cleaned coal	8.79	2.94	1.26	0.45	1.23	0.55	51.8	209.9	39.8	5.1	16.3	31.0	2.86	3.60	40.3	0.41	0.25	95.1	0.11	0.15	2.4	58.7
	Middlings	21.34	5.59	3.35	0.98	1.26	1.07	79.2	349.6	143.4	19.4	52.2	83.8	6.07	10.11	97.7	0.89	0.97	252.9	0.19	0.44	4.4	68.7
	Gangue	46.57	12.71	8.76	2.87	1.08	1.32	101.7	264.4	35.8	26.4	46.5	231.3	9.88	21.51	59.4	1.15	1.02	464.2	0.35	0.69	10.7	25.0
	Feed coal	20.64	5.78	2.75	1.68	1.35	0.95	112.5	298.7	67.3	17.8	41.1	98.3	6.19	11.43	76.6	0.59	0.57	208.4	0.18	0.28	4.5	83.9
3–6	Cleaned coal	8.08	2.63	1.06	0.35	1.22	0.60	22.9	249.9	48.6	4.5	15.3	28.1	1.90	3.06	39.7	0.36	0.26	69.7	0.12	0.23	3.2	10.5
	Middlings	18.46	5.12	2.69	1.09	1.34	0.77	56.4	198.9	49.7	9.5	24.8	53.6	4.84	6.59	52.9	1.85	0.57	179.0	0.17	0.33	6.5	15.8
	Gangue	43.89	12.35	7.48	3.53	1.34	1.41	105.6	243.8	39.1	18.9	39.1	173.9	9.52	19.06	49.4	1.04	1.03	454.7	0.33	0.63	10.7	43.7
	Feed coal	17.29	5.72	2.79	1.67	1.26	0.70	37.9	171.5	32.4	8.1	22.9	52.9	7.27	6.70	33.9	0.38	0.49	143.5	0.20	0.31	5.3	33.1
0.5–3	Cleaned coal	9.12	2.7	1.19	0.41	1.1	0.50	26.3	182.1	39.8	2.7	9.4	21.0	2.83	2.91	29.2	0.28	0.24	74.8	0.33	0.21	5.7	13.5
	Middlings	20.05	5.97	3.71	0.99	1.27	0.60	57.4	155.2	47.1	5.3	12.5	41.0	4.56	6.86	33.2	0.36	0.42	194.3	0.21	0.29	7.6	12.6
	Gangue	42.66	11.47	8.18	2.31	0.98	1.24	108.5	254.5	68.1	12.5	30.1	130.9	9.89	18.54	42.8	0.61	0.99	588.9	0.33	0.49	21.0	21.0
	Feed coal	19.15	6.35	2.83	2.38	1.14	0.65	53.9	162.8	27.6	6.4	18.1	45.3	6.31	6.32	29.6	0.27[a]	0.21[a]	118.1	0.17[a]	0.22	3.2[a]	32.4
< 0.5	Cleaned coal	9.6	2.9	0.81	0.86	1.22	0.43	28.8	164.7	33.9	5.1	17.9	28.7	6.79	3.14	32.4	0.15	0.01	75.7	0.15	0.23	4.6	31.3
	Middlings	20.97	6.68	2.96	2.58	1.14	0.47	33.4	122.0	22.9	6.8	20.7	42.0	11.78	4.05	23.1	0.29	0.09	114.7	0.31	0.39	7.8	36.4
	Gangue	44.05	15.17	8.25	6.82	0.1	0.58	45.9	138.5	18.8	10.9	36.4	73.4	15.71	8.14	21.8	0.58	0.24	237.7	0.32	0.74	7.7	21.9
	Feed coal	25.52	8.45	3.98	3.53	0.94	0.46	53.0	127.8	21.9	9.2	30.0	52.8	13.45	7.59	23.9	0.44	0.09	151.8	0.22	0.65	7.1	31.4

[a] The content of Cd, Sb, Hg, and Pb in feed coal with a size of 0.5–3 mm is lower than in coal preparation products because of the ion exchange between coal and gravity separation medium.

indicating that they are epigenetic in origin and may be influenced by low-temperature hydrothermal activity. Wang et al. (2006) indicated that epigenetic minerals can be effectively removed from coal by gravity separation. Flower marcasite was also noted in the Rongyang coals (Fig. 6f), indicating the Rongyang coal was influenced by low-temperature hydrothermal fluid.

The electron microprobe analysis indicated that U mainly occurs in clay minerals, anatase, and guadarramite (Fig. 8; Table 6). The U-bearing anatase coexists with clay minerals and contains trace amounts of Na, Mg, K, Ca, Zr, Nb, and I (Table 6: spots 1, 5, 6; Fig. 8a, b, c). The U-bearing clay minerals contain trace amounts of Na, Mg, Cl, S, K, Ca, Ti, Fe, Mn, Zr, I, and La (Table 6: spots 2, 3, 4, 7; Fig. 8b, c, d). The guadarramite coexists with the clay minerals (Fig. 8d; Table 6: spot 8), and contains trace Na, Mg, P, S, K, Ca, Mn, Zr, and Th.

The U-bearing minerals in the Rongyang coal are < 10 µm in size (Fig. 8). Wang et al. (2016) considered that fine-grained pyrite is generally < 10 µm in size. Ruppert et al. (2005) thought that coarse-grained pyrite is easy to remove from coal, but fine-grained pyrite is much more difficult to liberate. Thus, the U-bearing minerals are expected be difficult to be liberated as they are predominantly fine-grained minerals.

4.4. Origin of U in the Rongyang mine compared with adjacent regions

The Late Permian coals from the Rongyang Mine are characterized by a high content of sulfur and highly-elevated concentrations of a U-V-Cr-Co-Cu-Se-Mo assemblage, which is typical for some coals preserved within carbonate successions in southwestern China. According to Dai et al. (2008, 2013a, 2015, 2017b), the coals from Yanshan, Heshan, Guiding, and Yishan coalfields in southwestern China have similar sedimentary environments and are characterized by high organic sulfur and highly-elevated concentrations of a U-V-Cr-Co-Cu-Se-Mo assemblage. Moreover, coal beds from southwestern China are interbedded with limestones and are interpreted to have formed in an euxinic environment. The high U and other enriched trace elements (V, Se, Mo, Re) were derived from exfiltrational hydrothermal solutions during peat accumulation (Dai et al., 2015, 2016b). The Rongyang coals in this study are interpreted to have formed in a tidal flat (Xu and He, 2003), which are weak oxidizing environments and may have leaded to a relatively lower organic sulfur content than Yanshan, Heshan, Guiding, and Yishan coalfields in southwestern China. The U-V-Cr-Co-Cu-Se-Mo-rich hydrothermal solutions derived from Emeishan basalts (the Emeishan basalts overlie the Maokou Formation and are overlain by Longtan Formation) were diluted and flushed out by tidal forces during coal formation. As a result, uranium is enriched in the Rongyang coal, but its content is lower than those in Yanshan (153 µg/g), Heshan (111 µg/g), Guiding (211 µg/g), and Yishan (72.2 µg/g) coalfields. Therefore, the elevated U concentration is interpreted to have been derived from exfiltrational hydrothermal fluids during syngenesis or early diagenesis.

4.5. The partitioning of elements in different coal separation products

Percentages of ash and sulfur, concentrations of trace elements in coal separation products of different particle sizes are listed in Table 7. Hazardous elements Be, Cr, Co, Ni, Cu, Se, Mo, Cd, Sb, Ba, and U have the highest content in the fractions with a size of 6–13 mm (Fig. 9). The contents of F, As, Hg, Tl, and Pb decrease as particle size decreases, and they have the lowest contents in the fractions with a size of < 0.5 mm. Wang et al. (2006) and Wang and Qin (2011) showed that coarse-grained coals have more fractures that are often filled with minerals. Since minerals host most trace elements, coals with a size of 6–13 mm have relatively high trace-element concentrations.

Ash yield and sulfur content are high in gangue (Fig. 10), and they have the lowest content in the cleaned coal, suggesting that ash and sulfur can be effectively removed by gravity separation. In each particle
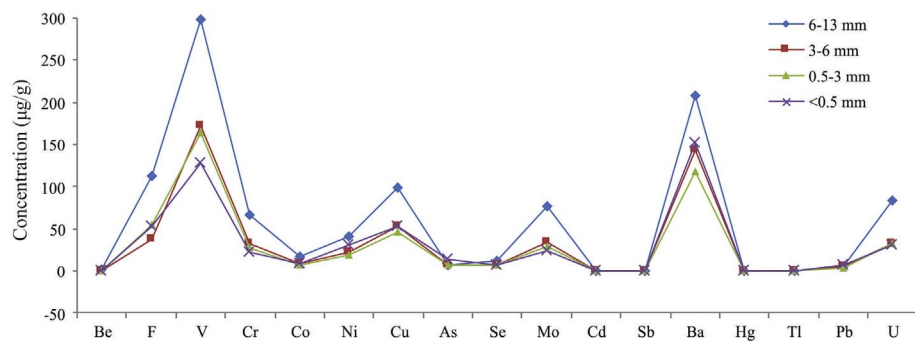
Fig. 9. Concentration of trace elements in the feed coal of different particle sizes.
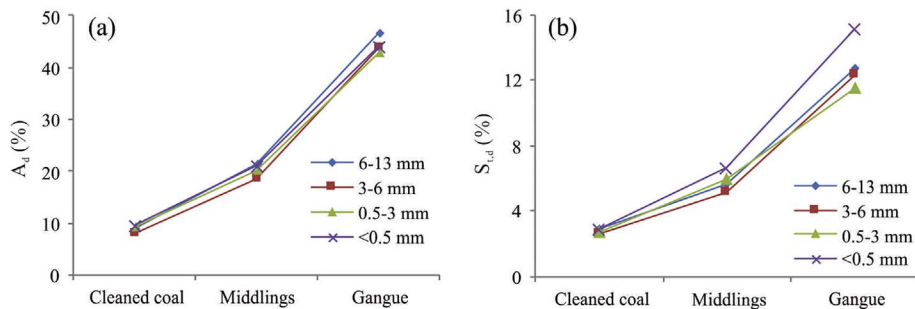

Fig. 10. Percentages (%) of ash and total sulfur in coal separation products of different particle sizes.
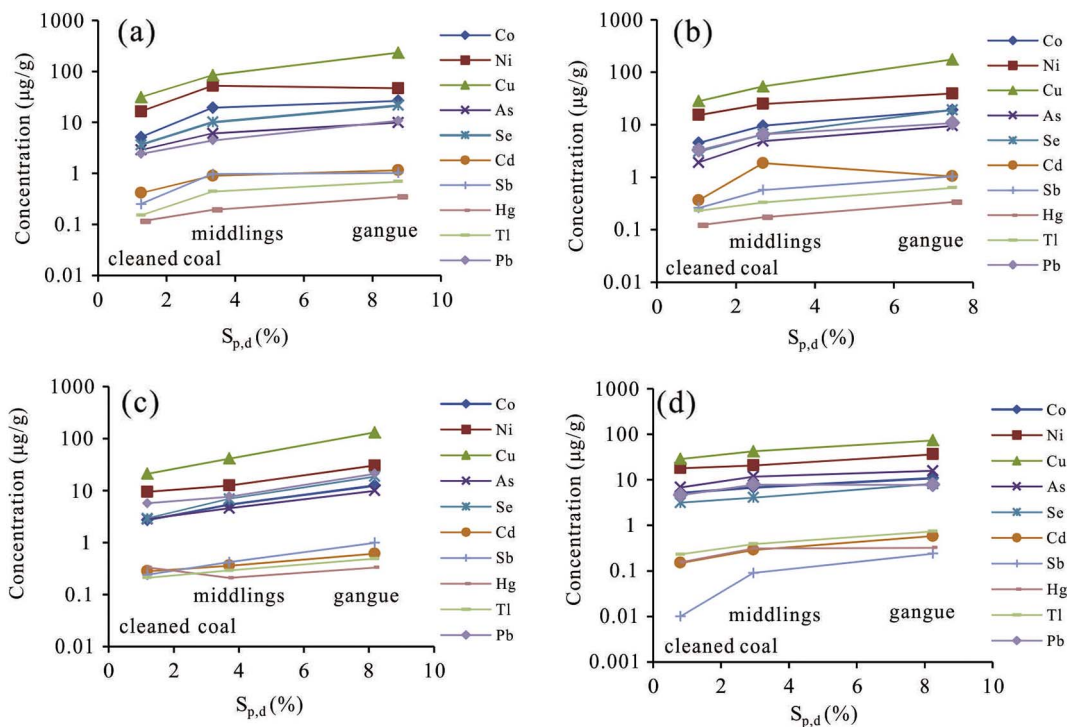

Fig. 11. Partitioning of Co, Ni, Cu, As, Se, Cd, Sb, Hg, Tl, and Pb in coal separation products of different particle sizes: (a) 6–13 mm; (b) 3–6 mm; (c) 0.5–3 mm; (d) < 0.5 mm (results on a whole coal dry air dried basis).

size fraction, uranium is irregularly distributed in the coal separation products. Moreover, uranium is enriched in cleaned coal in the size fraction 6–13 mm and < 0.5 mm (Fig. 13). XRD (Table 5) and EPMA (Fig. 8 and Table 6) show that U occurs in clay minerals, anatase, and guadarramite, as well as within organic materials. Concentrations of Co, Ni, Cu, As, Se, Cd, Sb, Hg, Tl, and Pb in cleaned coal, middlings, and gangue increase with increasing contents of $S_{p,d}$ (Fig. 11), indicating that these elements are associated with pyrite. Concentrations of Be, F and Ba in the different coal separation products increased with the increase of their corresponding A_d (Fig. 12), which indicates that Be, F,

and Ba are associated minerals. There were no distinct regular of V, Cr, and Mo in the cleaned coal, middlings, and gangue with their A_d (Fig. 13). In addition, the content of elements (V, Cr, and Mo) in each coal preparation product (cleaned coal, middlings and gangue) are higher than that in feed coal, suggesting that they evenly occurred in the minerals and organic portions.

4.6. The removability of hazardous elements

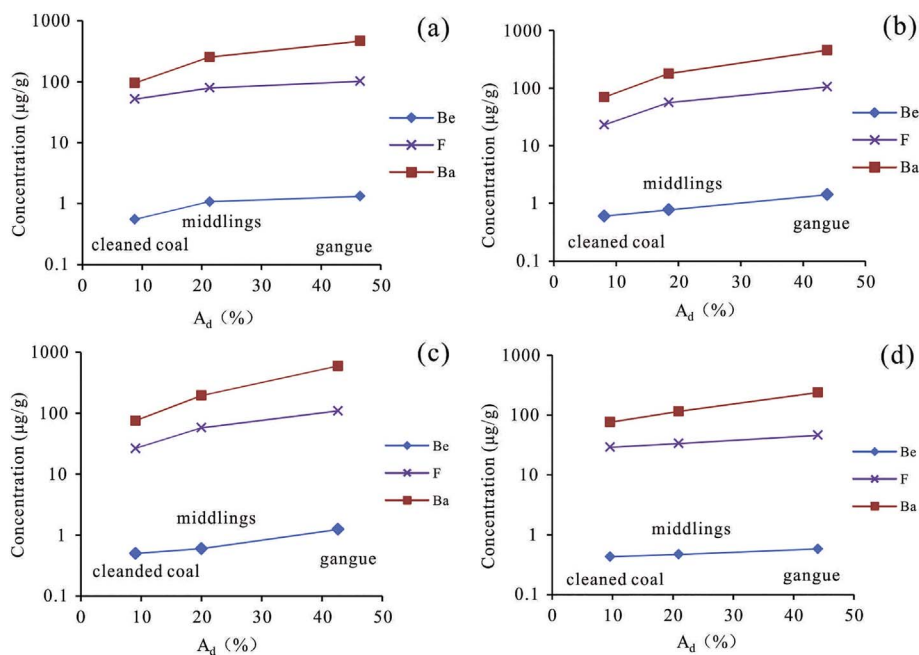In order to study the reduction degree of the elements during coal

Fig. 12. Partitioning of Be, F and Ba in coal separation products of different particle sizes: (a) 6–13 mm; (b) 3–6 mm; (c) 0.5–3 mm; and (d) < 0.5 mm (results on a whole coal air dried basis).
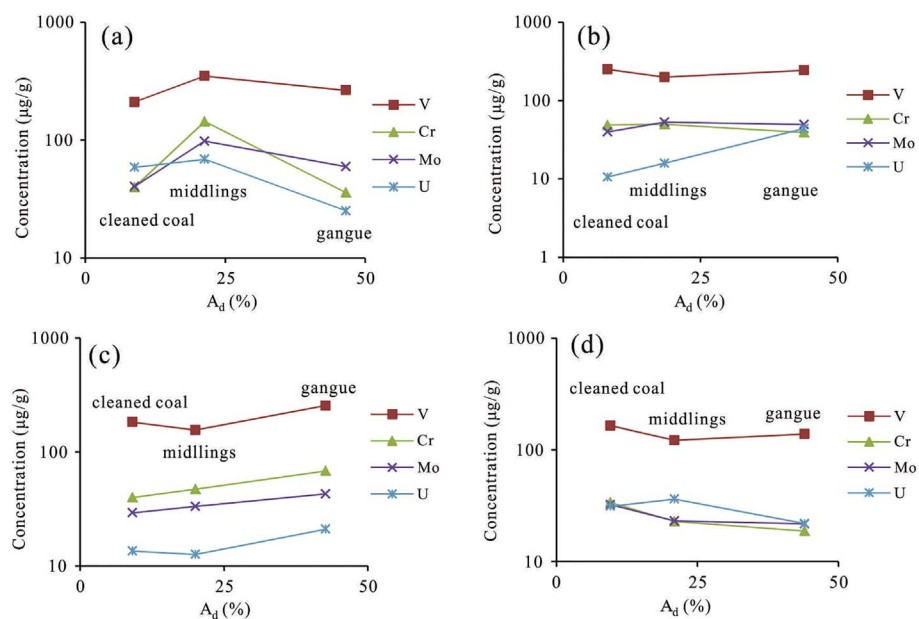

Fig. 13. Partitioning of V, Cr, Mo, and U in coal separation products of different particle sizes: (a) 6–13 mm; (b) 3–6 mm; (c) 0.5–3 mm; and (d) < 0.5 mm (results on a whole coal air dried basis).

preparation, the following equation (Wang et al., 2006) was used to calculate the removability.

$$R = (1 - c_{ij})/C_{ij} * 100\%$$

where R is the removability; c_{ij} is the content of element i in the cleaned coal or middlings with a particle size j; and C_{ij} is the content of element i in the feed coal with a particle size j.

The removability of ash, sulfur, and hazardous elements is listed in Table 8 and shown in Fig. 14. Ash, sulfur, and most of the hazardous elements have the highest removability in fractions with a particle size of < 0.5 mm, followed by 6–13 mm, and the lowest removability in fractions with particle sizes of 3–6 mm and 0.5–3 mm.

The removability values of U in fractions with particle sizes of 3–6 mm and 0.5–3 mm are 68.33% and 58.22%, respectively, higher than those of ash and sulfur. This demonstrates that U can be removed by desulphurization and demineralization. Uranium has a relatively low removability in fractions with particle sizes of 6–13 mm and < 0.5 mm.

A similar relationship is exhibited by As and Hg, which have the highest removability in fractions with a size of 3–6 mm. Fluorine has the highest removability in fractions with a size of 6–13 mm. Vanadium, Cr, Mo, and Ba could be removed efficiently in fractions with a particle size of 6–13 mm, but in the rest of the size fractions, they are difficult to remove (except Ba). Elements Co, Ni, Cu, Se, and Pb occurring in pyrite are more easily liberated in fractions with a size of 6–13 mm, whereas elements Cd, Sb, and Tl have the highest removability in coals with a size of < 0.5 mm. The removability values of lithophile elements are generally lower than those of sulphophile elements.

Uranium has the highest removability value (68.33%) and lowest content (10.5 μg/g) in fractions with a size of 3–6 mm compared to other size fractions. Compared to the world hard coals (Ketris and Yudovich, 2009), uranium is still enriched in the cleaned coal (Fig. 15), indicating that U can be reduced by gravity coal separation, but cannot decrease to the content in world hard coal due to U mainly occurring in the organic portions and fine-grained minerals. Vanadium, Cr, and Mo

Table 8
Removability (%) of ash, sulfur, and hazardous elements in cleaned coal and middling.

| Size grade	6–13 mm		3–6 mm		0.5–3 mm		< 0.5 mm	
Coal preparation products	Cleaned coal	Middlings	Cleaned coal	Middlings	Cleaned coal	Middlings	Cleaned coal	Middlings
A_d	57.41	− 3.39	53.27	− 6.77	52.38	− 4.70	62.38	17.83
$S_{t.d}$	49.21	3.25	53.99	10.53	57.48	5.96	65.66	21.01
$S_{p.d}$	54.05	− 21.77	61.95	3.42	58.10	− 30.91	79.59	25.80
$S_{s.d}$	73.23	41.30	79.27	34.88	82.84	58.54	75.51	26.97
$S_{o.d}$	9.22	6.99	2.83	− 6.05	3.11	− 11.40	− 30.06	− 21.80
Be	41.83	− 12.92	14.29	− 9.60	23.94	7.94	5.84	− 2.68
F	53.95	29.56	39.48	− 48.69	51.28	− 6.34	45.56	36.91
V	29.75	− 17.04	− 45.71	− 15.99	− 11.88	4.68	− 28.92	4.50
Cr	40.84	− 113.10	− 50.05	− 53.42	− 44.17	− 70.78	− 54.62	− 4.33
Co	71.26	− 8.72	44.56	− 17.71	58.24	17.42	44.14	26.11
Ni	60.26	− 26.82	33.17	− 8.55	47.96	30.73	40.28	31.08
Cu	68.51	14.79	46.88	− 1.27	53.63	9.62	45.54	20.40
As	53.71	1.85	73.88	33.49	55.09	27.68	49.53	12.44
Se	68.50	11.49	54.24	1.57	54.01	− 8.49	58.69	46.67
Mo	47.34	− 27.57	− 17.14	− 55.89	1.51	− 11.95	− 35.23	3.51
Cd	30.04	− 52.64	5.19	− 388.68	− 1.81	− 32.17	65.37	35.03
Sb	56.87	− 69.14	47.59	− 15.29	− 15.02	− 99.88	94.13	− 8.11
Ba	54.37	− 21.32	51.42	− 24.74	36.63	− 64.63	50.14	24.43
Hg	36.09	− 7.19	39.66	14.04	− 96.84	− 23.38	28.30	− 44.33
Tl	45.67	− 56.02	26.10	− 5.06	2.70	− 30.90	64.47	39.12
Pb	45.86	0.74	38.46	− 24.36	− 78.95	− 139.45	35.29	− 9.72
U	30.01	18.09	68.33	52.23	58.22	61.05	0.14	− 16.14
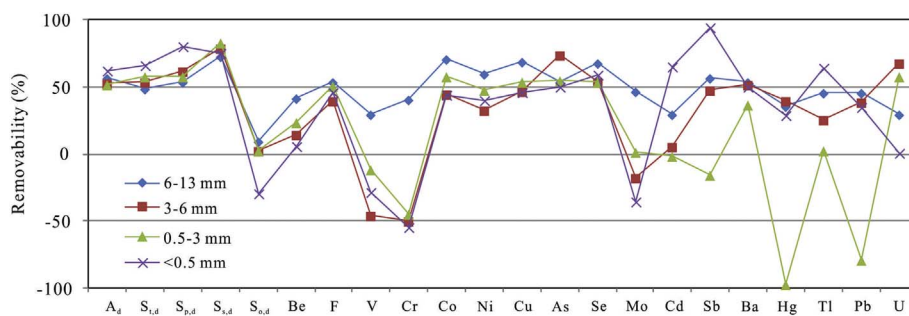
Fig. 14. Removability of ash and elements in cleaned coal.
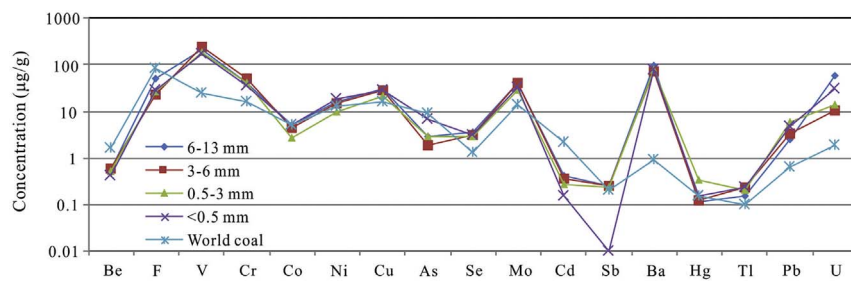

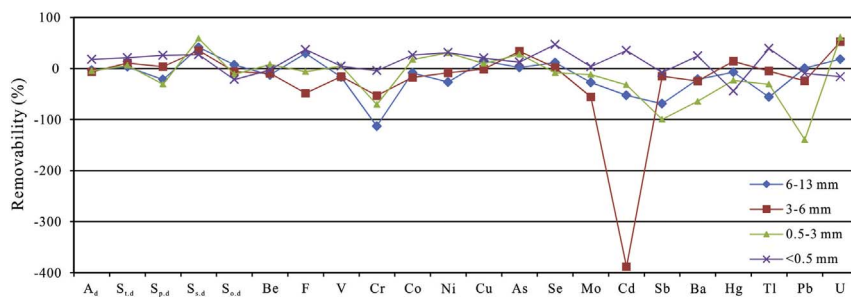**Fig. 15.** Concentrations of hazardous elements in cleaned coal and world hard coals.

Fig. 16. Removability of ash and elements in middlings.

Table 9
The concentrations of U in cleaned coal and their ash with different particle sizes.

Particle size (mm)	Ash yield (%)	Content of U in coal (μg/g)	Percentage of U in ash (%)
6–13	8.79	58.7	0.067%
3–6	8.08	10.5	0.013%
0.5–3	9.12	13.5	0.015%
< 0.5	9.60	31.3	0.033%

cannot be removed by gravity coal separation. The content of most element (except Be, As, Cd, and Hg) in cleaned coal is still higher than those in world hard coals.

The removability of ash, sulfur, and hazardous elements in middlings is listed in Table 8 and shown in Fig. 16. Ash and sulfur have the highest removability in fractions with a size of < 0.5 mm. As with the cleaned coal, uranium has the highest removability in fractions with particle sizes of 3–6 mm and 0.5–3 mm (52.23% and 61.05%, respectively); however, uranium has the lowest removability in coals with sizes of 6–13 mm and < 0.5 mm. The removal efficiency of V, Cr, and Mo are poor in all size-fractions. The removability of Se is highest in fractions with a size of < 0.5 mm. The removability of other elements in middlings is low or negative, and the removal efficiency is better than the fractions with sizes of 3–6 mm, 3–0.5 mm, and < 0.5 mm.

4.7. The economic evaluation of uranium

The enriched trace elements will be expected to concentrate in coal ash, and therefore, uranium can be extracted from combustion products of cleaned coal. In order to evaluate the economic significance of U in Rongyang coal, the percentage of U in the ash from cleaned coal is calculated (Table 9). According to Chinese Reference Manual of Industrial Requirements for Ores (1987), the cut-off and industrial grade for U in coal are 0.03% and 0.05%, respectively. From Table 9, the percentages of U in the ash from cleaned coal with particle sizes of 6–13 mm and < 0.5 mm are higher than industrial grade and cut-off grade, respectively, however, the percentages of U in ash with particle sizes of 3–6 mm and 0.5–3 mm are lower than cut-off grade. In conclusion, the ash from coarse-sized and fine-grained cleaned coal could potentially be used for industrial extraction of U.

5. Conclusions

(1) The Late Permian coal from the Rongyang Mine in southwestern China is characterized by high sulfur (5.44%) and high concentrations of the trace elements U (70.5 μg/g), V (283 μg/g), Cr (63.2 μg/g), Co (12.8 μg/g), Cu (59.5 μg/g), Se (5.28 μg/g), and Mo (87.5 μg/g). The minerals in the Rongyang coals are mainly composed of quartz, pyrite, marcasite, calcite, anatase, illite, and kaolinite, along with trace amounts of coquimbite, bassanite, roemerite, gypsum, dolomite, rutile, and siderite. Most of the minerals, including quartz, pyrite, marcasite, calcite, anatase, and clays, can be effectively liberated from the cleaned coal through gravity separation.

(2) Elements U, V, Cr, Co, Cu, Se, and Mo in Rongyang coals are derived from exfiltrational hydrothermal fluids in the stage of syngenesis or early diagenesis. These elements are mainly associated with the inorganic components within the coal, such as clay minerals, pyrite, anatase, and guadarramite, although there is some evidence they may also occur within the organic material as well. In addition, a portion of Se occurs in epigenetic pyrite. The major occurrence of Co, Ni, Cu, As, Cd, Sb, Hg, Tl, and Pb is within pyrite. Be, F, and Ba occur in inorganic components.

(3) The Rongyang coal is influenced by epigenetic hydrothermal activity and the minerals that are epigenetic in origin are easily liberated during coal cleaning. Ash, sulfur, and most of the hazardous materials have the highest removability in the cleaned coal in the fractions with particle sizes of 6–13 mm and < 0.5 mm; however, ash, sulfur, and most of the hazardous materials are easy to remove in middlings with a size of < 0.5 mm. The removability of ash, sulfur, and hazardous elements in cleaned coal is much higher than in the middlings.

(4) Uranium has the highest removability (68%) and lowest concentration (10.5 μg/g) in the fractions with a size of 3–6 mm compared to the other size fractions, but it cannot be fully removed by gravity separation. The U concentration in the cleaned coal is still much higher than the average value of hard coals for the world because of its association with organic components and fine-grained minerals, and the ash from cleaned coal with particle size of 6–13 mm and < 0.5 mm could be used for industrial extraction of uranium. Elements Co, Ni, Cu, As, Se, Cd, Sb, Hg, Tl, and Pb, which are associated with epigenetic pyrite, and elements Be, F, and Ba, which occur in inorganic minerals, have relative high removability, whereas V, Cr, and Mo, which is evenly distributed in minerals and organic material, are difficult to be removed.

Appendix A. Supplementary data

Supplementary data to this article can be found online at https://doi.org/10.1016/j.gexplo.2017.10.022.

References

ASTM Standard D2492-02, 2002. Test Methods for Forms Sulfur in the Analysis Sample of Coal and Coke. ASTM International, West Conshohocken, PA (Reapproved 2007).

ASTM Standard D3173-11, 2011. Test Method for Moisture in the Analysis Sample of Coal and Coke. ASTM International, West Conshohocken, PA.

ASTM Standard D3174-11, 2011. Annual Book of ASTM Standards. Test Method for Ash in the Analysis Sample of Coal and Coke. ASTM International, West Conshohocken, PA.

ASTM Standard D3175-11, 2011. Test Method for Volatile Matter in the Analysis Sample of Coal and Coke. ASTM International, West Conshohocken, PA.

ASTM Standard D3177-02, 2002. Test Methods for Total Sulfur in the Analysis Sample of Coal and Coke. ASTM International, West Conshohocken, PA (Reapproved 2007).

ASTM Standard D388-12, 2012. Standard Classification of Coals by Rank. ASTM International, West Conshohocken, PA.

ASTM Standard D5987-96, 2002. Standard Test Method for Total Fluorine in Coal and Coke by Pyrohydrolytic Extraction and Ion Selective Electrode or Ion Chromatograph Methods. ASTM International, West Conshohocken, PA.

Chen, J., Chen, P., Yao, D., Huang, W., Tang, S., Wang, K., Liu, W., Hu, Y., Li, Q., Wang, R., 2017. Geochemistry of uranium in Chinese coals and the emission inventory of coal-fired power plants in China. Int. Geol. Rev. http://dx.doi.org/10.1080/00206814.2017.1295284.

Cheng, W., Zhang, Q., Yang, R., Tian, Y., 2013. Occurrence modes and cleaning potential of sulfur and some trace elements in a high-sulfur coal from Pu'an coalfield, SW Guizhou, China. Environ. Earth Sci. 72 (1), 35–46.

China Coal Geology Bureau, 1996. Sedimentary Environments and Coal Accumulation of Late Permian Coal Formation in Western Guizhou, Southern Sichuan, and Eastern Yunnan, China. Chongqing University Press, Chongqing, pp. 156–216 (in Chinese with English abstract).

Chou, C.-L., 2012. Sulfur in coals: a review of geochemistry and origins. Int. J. Coal Geol. 100, 1–13.

Dai, S., Finkelman, R.B., 2017. Coal as a promising source of critical elements: progress and future prospects. Int. J. Coal Geol. http://dx.doi.org/10.1016/j.coal.2017.06.005.

Dai, S., Chou, C.-L., Yue, M., Luo, K., Ren, D., 2005. Mineralogy and geochemistry of a Late Permian coal in the Dafang Coalfield, Guizhou, China: influence from siliceous and iron-rich calcic hydrothermal fluids. Int. J. Coal Geol. 61, 241–258.

Dai, S., Zeng, R., Sun, Y., 2006. Enrichment of arsenic, antimony, mercury, and thallium in a Late Permian anthracite from Xingren, Guizhou, Southwest China. Int. J. Coal Geol. 66, 217–226.

Dai, S., Ren, D., Zhou, Y., Chou, C.-L., Wang, X., Zhao, L., Zhu, X., 2008. Mineralogy and geochemistry of a super high-organic-sulfur coal, Yanshan Coalfield, Yunnan, China:

evidence for a volcanic ash component and influence by submarine exhalation. Chem. Geol. 255, 182–194.

Dai, S., Wang, X., Zhou, Y., Hower, J.C., Li, D., Chen, W., Zhu, X., 2011. Chemical and mineralogical compositions of silicic, mafic, and alkali tonsteins in the late Permian coals from the Songzao Coalfield, Chongqing, Southwest China. Chem. Geol. 282 (1–2), 29–44.

Dai, S., Ren, D., Chou, C.-L., Finkelman, R.B., Seredin, V.V., Zhou, Y., 2012. Geochemistry of trace elements in Chinese coals: a review of abundances, genetic types, impacts on human health, and industrial utilization. Int. J. Coal Geol. 94 (3), 3–21.

Dai, S., Zhang, W., Seredin, V.V., Ward, C.R., Hower, J.C., Song, W., Wang, X., Li, X., Zhao, L., Kang, H., Zheng, L., Wang, P., Zhou, D., 2013a. Factors controlling geochemical and mineralogical compositions of coals preserved within marine carbonate successions: a case study from the Heshan Coalfield, southern China. Int. J. Coal Geol. 109-110 (2), 77–100.

Dai, S., Zhang, W., Ward, C.R., Seredin, V.V., Hower, J.C., Li, X., Song, W., Wang, X., Kang, H., Zheng, L., Wang, P., Zhou, D., 2013b. Mineralogical and geochemical anomalies of late Permian coals from the Fusui Coalfield, Guangxi Province, southern China: influences of terrigenous materials and hydrothermal fluids. Int. J. Coal Geol. 105, 60–84.

Dai, S., Seredin, V.V., Ward, C.R., Hower, J.C., Xing, Y., Zhang, W., Song, W., Wang, P., 2015. Enrichment of U-Se-Mo-Re-V in coals preserved within marine carbonate successions: geochemical and mineralogical data from the Late Permian Guiding Coalfield, Guizhou, China. Mineral. Deposita 50, 159–186.

Dai, S., Chekryzhov, I.Y., Seredin, V.V., Nechaev, V.P., Graham, I.T., Hower, J.C., Ward, C.R., Ren, D., Wang, X., 2016a. Metalliferous coal deposits in East Asia (Primorye of Russia and South China): a review of geodynamic controls and styles of mineralization. Gondwana Res. 29, 60–82.

Dai, S., Yan, X., Ward, C.R., Hower, J.C., Zhao, L., Wang, X., Zhao, L., Ren, D., Finkelman, R.B., 2016b. Valuable elements in Chinese coals: a review. Int. Geol. Rev. http://dx.doi.org/10.1080/00206814.2016.1197802.

Dai, S., Xie, P., Jia, S., Ward, C.R., Yan, X., French, D., 2017a. Enrichment of U-Re-V-Cr-Se and rare earth elements in the Late Permian coals of the Moxinpo Coalfield, Chongqing, China: genetic implications from geochemical and mineralogical data. Ore Geol. Rev. 80, 1–17.

Dai, S., Xie, P., Ward, C.R., Yan, X., Guo, W., French, D., Graham, I.T., 2017b. Anomalies of rare metals in Lopingian super-high-organic-sulfur coals from the Yishan Coalfield, Guangxi, China. Ore Geol. Rev. 88, 235–250.

Diehl, S.F., Goldhaber, M.B., Koenig, A.E., Lowers, H.A., Ruppert, L.F., 2012. Distribution of arsenic, selenium, and other trace elements in high pyrite Appalachian coals: evidence for multiple episodes of pyrite formation. Int. J. Coal Geol. 94, 238–249.

Duan, P., Wang, W., Liu, X., Qian, F., Sang, S., Xu, S., 2017. Distribution of As, Hg and other trace elements in different size and density fractions of the Reshuihe high-sulfur coal, Yunnan Province, China. Int. J. Coal Geol. 173, 129–141.

Feng, L., Lu, M., Liu, H., Jia, J., Su, L., 2008. Study on the transport of mercury during coal preparation. Clean Coal Technol. 14 (4), 16–18 (in Chinese).

Finkelman, R.B., Tian, L., 2017. The health impacts of coal use in China. Int. Geol. Rev. http://dx.doi.org/10.1080/00206814.2017.1335624.

GB/T 15224.1-2004 (National Standard of P.R. China), 2004. Classification for Quality of Coal. Part 1: Ash. (in Chinese).

GB/T 15224.2-2004 (National Standard of P.R. China), 2004. Classification for Quality of Coal. Part 2: Sulfur Content. (in Chinese).

Gerald, H., Luttrell, J.N., Yoon, R.H., 2000. An evaluation of coal preparation technologies for controlling trace element emissions. Fuel Process. Technol. 65–66, 407–422.

Hu, J., Zheng, B., Wang, M., Finkelman, R.B., 2005. Distribution and forming cause of sulphur in Chinese coals. Coal Convers. 28 (4), 5–10 (in Chinese).

Huang, W., Tang, X., 2002. Uranium, thorium and other radionuclides in coal of China. Coal Geol. China 14 (s1), 55–63 (in Chinese).

Ketris, M.P., Yudovich, Y.E., 2009. Estimations of Clarkes for carbonaceous biolithes: world average for trace element contents in black shales and coals. Int. J. Coal Geol. 78, 135–148.

Kolker, A., Senior, C., Alphen, C.V., Koenig, A., Geboy, N., 2016. Mercury and trace element distribution in density separates of a South African Highveld (#4) coal: implications for mercury reduction and preparation of export coal. Int. J. Coal Geol. 170, 7–13.

Li, D., Tang, Y., 2005. Geological genesis of coal geochemical anomalies of the Late Permian coals from the Qinglong Coalfield in Western Guizhou, China. Geol. Rev. 51 (2), 163–168 (in Chinese).

Li, X., Dai, S., Zhang, W., Li, T., Zheng, X., Chen, W., 2014. Determination of As and Se in coal and coal combustion products using closed vessel microwave digestion and collision/reaction cell technology (CCT) of inductively coupled plasma mass spectrometry (ICP-MS). Int. J. Coal Geol. 124, 1–4.

Luo, K., Li, H., Niu, C., 2008. Fluorine and arsenic pollution route of grain in Yunnan-Guizhou "coal-burning" endemic fluorosis area. Geol. Rev. 56 (2), 289–298 (in Chinese).

Man, C.K., Jacobs, J., Gibbins, J.R., 1998. Selective maceral enrichment of the Liddell seam, upper Hunter Valley, New South Wales. Int. J. Coal Geol. 56, 215–227.

Office of Mineral Resources Committee in China, 1987. Reference Manual of Industrial Requirements for Ores. Geologied Publishing House (in Chinese).

Ruppert, L.R., Hower, J.C., Eble, C.F., 2005. Arsenic-bearing pyrite and marcasite in the Fire Clay coal bed, Middle Pennsylvanian Breathitt Formation, eastern Kentucky. Int. J. Coal Geol. 63, 27–35.

Wang, L., 2007. The study on removal of trace elements in coal by coal preparation. Clean Coal Technol. 13 (3), 13–17 (in Chinese).

Wang, W., Qin, Y., 2011. Partitioning of Hazardous Elements and Minerals during Coal Cleaning. China University of Mining and Technology Press (in Chinese).

Wang, M., Zheng, B., Finkelman, R.B., Hu, J., Wu, D., Li, S., 2005. Relationship between occurrence m ode of arsenic in coal and its washing rate. J. Fuel Chem. Technol. 33 (2), 253–256.

Wang, W., Qin, Y., Sang, S., Jiang, B., Guo, Y., Zhu, Y., Fu, X., 2006. Partitioning of minerals and elements during preparation of Taixi coal, China. Fuel 85 (1), 57–67.

Wang, W., Qin, Y., Wei, C., Li, Z., Guo, Y., Zhu, Y., 2008. Partitioning of elements and macerals during preparation of Antaibao coal. Int. J. Coal Geol. 68 (3–4), 223–232.

Wang, W., Qin, Y., Wang, J., Li, J., 2009. Partitioning of hazardous trace elements during coal preparation. Procedia Earth Planet. Sci. 1 (1), 838–844.

Wang, X., Feng, Q., Fang, T., Liu, J., Liu, G., 2015. Geochemical characteristics of uranium in medium to high sulfur coals from Eastern Yunnan, China. J. China Coal Soc. 40 (10), 2451–2457 (in Chinese).

Wang, W., Sang, S., Bian, Z., Duan, P., Qian, F., Lei, S., Qin, Y., 2016. Fine-grained pyrite in some Chinese coals. Energy Explor. Exploit. 34 (4), 543–560.

Xu, B., He, M., 2003. Guizhou Coalfield Geology[M]. China University of Mining and Technology Press, Xuzhou (in Chinese).